

Estimating the Number of Clusters via Normalized Cluster Instability

Jonas M. B. Haslbeck

Psychological Methods Group, University of Amsterdam
and

Dirk U. Wulff

Center for Cognitive and Decision Science, University of Basel
Center for Adaptive Rationality, Max Planck Institute for Human Development, Berlin

March 10, 2022

Abstract

We improve existing instability-based methods for the selection of the number of clusters k in cluster analysis by normalizing instability. In contrast to existing instability methods which only perform well for bounded sequences of small k , our method performs well across the whole sequence of possible k . In addition, we compare for the first time model-based and model-free variants of k selection via cluster instability and find that their performance is similar. We make our method available in the R-package `cstab`.

Keywords: cluster analysis, k-means, stability, resampling

1 Introduction

A central problem in cluster analysis is selecting the appropriate number of clusters k . To develop a method that identifies the true number of clusters k^* , one requires a formal definition for what a 'good clustering' is. Different definitions have been proposed and it is generally accepted that the appropriate definition depends on the clustering problem at hand (see e.g. Friedman *et al.*, 2001; Hennig, 2015).

Most definitions in the literature define the quality of a clustering in terms of a distance metric between the clustered objects. These methods select k by trading-off a function of this distance metric against the number of k . The most commonly used distance metric is the average (across clusters) within-cluster dissimilarity $W(k)$, which is the average dissimilarity between all object-pairs within the same cluster. When selecting the k based on this metric one assumes that $W(k)$ shows a 'kink' at $k = k^*$, because $k > k^*$ one splits homogeneous clusters which leads to smaller improvements in $W(k)$. All methods in this class, in one way or another, aim to identify this 'kink'. Two other methods are the Gap statistic (Tibshirani *et al.*, 2001) and the Jump statistic (Sugar and James, 2011). Related metrics are the Silhouette statistic (Rousseeuw, 1987), which is a measure of cluster separation rather than variance, and a refinement thereof, the Slope statistic (Fujita *et al.*, 2014).

Another approach, which is the focus of this paper, defines a good clustering in terms of its *stability* against small perturbations of the data. Correspondingly, stability-based methods select the k yielding the most stable clustering. Stability-based methods are attractive because they do not require a metric for the distance between objects and have been shown to perform at least as well as state-of-the-art distance-based methods (Ben-Hur *et al.*, 2001; Tibshirani and Walther, 2005; Hennig, 2007; Wang, 2010; Fang and Wang, 2012).

In the present paper, we show that two previously proposed stability-based approaches, the *model-based* approach (Fang and Wang, 2012) and the *model-free* approach (Ben-Hur *et al.*, 2001), lead to incorrect estimates \hat{k} when the list of candidate k is not restricted to a small set, e.g., $k \in \{2, 3, \dots, 10\}$. To address this problem, we propose a normalization of the instability path which allows to identify k^* without restricting k to small values. Moreover, we report the first comparison of model-based and model-free approaches to clustering instability and find that they perform similarly well. Finally, we make our method available in the R-package `cstab`,

which is available on The Comprehensive R Archive Network (CRAN).

2 Clustering Instability

A clustering $\psi(\cdot)$ is stable if it is robust against small perturbations of the data. That is, if two objects X_1, X_2 are assigned to the same cluster by the clustering $\psi(X)$ based on the original data X , then stable clusterings also assign the two objects to the same cluster in a clustering $\psi(\tilde{X})$ based on a perturbed data \tilde{X} . In this section we formalize this idea similar to Wang (2010) using the terms *clustering distance* and *clustering instability*.

Let $\mathbf{X} = \{X_1, \dots, X_n\} \in \mathbb{R}^{n \times p}$ be n samples from a p -dimensional random vector from an unknown distribution \mathcal{P} . We define a clustering $\psi : \mathbb{R}^{n \times p} \mapsto \{1, \dots, K\}^n$ as a mapping from a configuration $X_i \in \mathbb{R}^p$ to a cluster assignment $k \in \{1, \dots, K\}$. A clustering algorithm $\Psi(\mathbf{X}, k)$ learns such a mapping from data.

Definition 1 (Clustering Distance). The distance between any pair of clusterings $\psi_a(X)$ and $\psi_b(X)$ is defined as

$$d(\psi_a(X^0), \psi_b(X^0)) = |\mathbb{I}_{\{\psi_a(X_1)=\psi_a(X_2)\}} - \mathbb{I}_{\{\psi_b(X_1)=\psi_b(X_2)\}}|$$

where $X^0 = \{X_1, X_2\}$ is a fixed vector containing the two objects X_1, X_2 and $\mathbb{I}_{\{E\}}$ is the indicator function for the event E .

Note that the distance $d(\psi_a(X_1), \psi_b(X_2)) \in [0, 1]$ is equal to 0 if the two objects X_1, X_2 are in the same cluster in the clustering ψ_a and also in the same cluster in the other clustering ψ_b . Conversely, the distance is equal to 1 if the pair of objects that is in the same cluster in clustering ψ_a is *not* in the same cluster in clustering ψ_b . Alternatively we can express the clustering distance as the probability that two clusterings disagree in whether two objects X_1, X_2 are in the same cluster

$$\begin{aligned} d(\psi_a, \psi_b) = & P[\psi_a(X_1) = \psi_a(X_2), \psi_b(X_1) \neq \psi_b(X_2)] \\ & + P[\psi_a(X_1) \neq \psi_a(X_2), \psi_b(X_1) = \psi_b(X_2)]. \end{aligned} \tag{1}$$

We now use the notion of clustering distance to define clustering instability.

Definition 2 (Clustering instability). We define the clustering instability of clustering algorithm $\Psi(X, k)$ as

$$s(\Psi, \mathbf{X}, k) = \mathbb{E}_{\mathcal{P}} \left[\frac{1}{n(n-1)/2} \sum_{i=1, j=i+1}^n d(\psi(\mathbf{X}), \psi(\tilde{\mathbf{X}})) \right]$$

where \mathbf{X} is a vector with n objects drawn from an unknown distribution \mathcal{P} , $\tilde{\mathbf{X}}$ is a perturbed version of \mathbf{X} , and the expectation is taken with respect to \mathcal{P} .

Note that $s(\Psi, \mathbf{X}, k) \in [0, 1]$, because for a vector \mathbf{X}^0 we take the average clustering distance over all unequal pairs of objects in \mathbf{X}^0 . Now, the optimal number of clusters k^* can be estimated by minimizing the cluster instability as a function of k

$$\hat{k} = \arg \min_{2 \leq k \leq n} s(\Psi, \mathbf{X}, k). \quad (2)$$

In practice \mathcal{P} is unknown and we therefore cannot draw a pair of samples from this distribution. Instead we take two bootstrap samples from the original data \mathbf{X} to compute the clustering instability. In almost all situations the two bootstrap samples contain a different set of objects. From this follows that the clusterings computed from the two bootstrap samples only provide a cluster assignment for the objects that are contained in the respective bootstrap sample. But in order to compute clustering instability, we need a cluster assignment for each object (in the original data set) from both clusterings. The model-based and the model-free approach, which we describe in the next two sections, solve this problem in different ways.

3 Model-Based Clustering Instability

The model-based clustering approach uses clustering algorithms $\Psi(\cdot, k)$ that learn a partitioning of the p -dimensional object space into k non-empty subsets (clusters), for each of the two perturbed data sets $\tilde{\mathbf{X}}_1, \tilde{\mathbf{X}}_2$. These partitions can then be used to assign unseen objects to the clusters. One example for a model-based clustering algorithm is the k-means algorithm, which partitions the p -dimensional feature space in k Voroni cells (Hartigan, 1975).

The model-based approach was first described as a cross validation (CV) scheme (Tibshirani and Walther, 2005; Wang, 2010), however, here we present the algorithm for the non-parametric

bootstrap, which has been shown to perform better than CV (Fang and Wang, 2012).

1. Take bootstrap samples $\tilde{\mathbf{X}}_a, \tilde{\mathbf{X}}_b$ from the empirical distribution \mathbf{X}
2. Compute clustering assignments $\psi_a(\tilde{\mathbf{X}}_a), \psi_b(\tilde{\mathbf{X}}_b)$ using the clustering algorithm $\Psi(\cdot, k)$
3. Use the clusterings ψ_a, ψ_b to compute assignments $\psi_a(\mathbf{X}), \psi_b(\mathbf{X})$ on the original data \mathbf{X}
4. Use $\psi_a(\mathbf{X}), \psi_b(\mathbf{X})$ to compute the clustering instability as in (2)

Repeat 1-4 B times and return the average instability $\bar{s}(\Psi, \mathbf{X}, k) = B^{-1} \sum_{i=1}^B s_i(\Psi, \mathbf{X}, k)$.

Algorithm 1: Model-Based Clustering Instability

The model-based approach can also be used for spectral clustering (Ng *et al.*, 2002) using the method described in Bengio *et al.* (2003). However, because of the requirement for a full partitioning of the object space, the approach is not readily applicable to, for instance, hierarchical clustering (Friedman *et al.*, 2001). To nonetheless apply the above procedure, one would have to implement an additional classifier (e.g. k nearest neighbors) trained on the initial clusterings to predict cluster assignment for new object. However, this issue can be sidestepped using the model-free approach described in the next section.

4 Model-Free Clustering Instability

The model-free approach (Ben-Hur *et al.*, 2001) uses any clustering algorithm $\Psi(\cdot, k)$ to compute two clusterings on the two perturbed datasets $\tilde{\mathbf{X}}_a, \tilde{\mathbf{X}}_b$. Clustering instability is then assessed only for the intersection set $\tilde{\mathbf{X}}_{a \cap b} = \tilde{\mathbf{X}}_a \cap \tilde{\mathbf{X}}_b$, i.e., the set of objects that are shared across both datasets. Remember that the problem of assigning unseen objects arises from objects that are unique to one of the datasets.

1. Take bootstrap samples $\tilde{\mathbf{X}}_a, \tilde{\mathbf{X}}_b$ from the empirical distribution \mathbf{X}
2. Compute clustering assignments $\psi_a(\tilde{\mathbf{X}}_a), \psi_b(\tilde{\mathbf{X}}_b)$ using the clustering algorithm $\Psi(\cdot, k)$
3. Take the intersection $\tilde{\mathbf{X}}_{a \cap b} = \tilde{\mathbf{X}}_a \cap \tilde{\mathbf{X}}_b$
4. Use $\psi_a(\tilde{\mathbf{X}}_{a \cap b}), \psi_b(\tilde{\mathbf{X}}_{a \cap b})$ to compute the clustering instability as in (2)

Repeat 1-4 B times and return the average instability $\bar{s}(\Psi, \mathbf{X}, k) = B^{-1} \sum_{i=1}^B s_i(\Psi, \mathbf{X}, k)$.

Algorithm 2: Model-Free Clustering Instability

Because no unseen objects need to be assigned, Algorithm 2 can use any *any* clustering algorithm $\Psi(\cdot, k)$. A potential prize for this flexibility is that Algorithm 2 compared to Algorithm 1 computes clustering instability only on approximately 40 %¹ of the original data, implying that more bootstrap comparisons may be needed to achieve equal performance.

5 Normalized Clustering Instability

In this section we describe how to normalize clustering instability (2) for both the model-based and the model-free approaches to remedy a shortcoming of current stability-based methods: Clustering instability (as defined in 2) has the undesirable property that it trivially decreases with increasing k . To see this, consider the clustering distance in (1): this distance can only be nonzero if a pair of objects X_1, X_2 can be assigned to the same cluster, that is, if $k < n$. Now, considering the whole range of k , we will show that the probability that two objects X_1, X_2 are by chance assigned to the same cluster $p[\psi(X_1) = \psi(X_2)]$ decreases with the number of clusters k , and therefore also $s(\Psi, X, k)$. This continues until $k = n$, at which point $p[\psi(X_1) = \psi(X_2)]$ and $s(\Psi, X, k)$ have to be equal to 0. This means that for an completely unconstrained set of candidate k , \hat{k} will necessarily overestimate k^* .

In Figure 1 we illustrate this issue using the same clustering problem as in Fang and Wang (2012): the unnormalized methods show an instability path with a local minimum at $k^* = 3$. However, from $k = 6$ on the clustering instability begins to decrease. The dashed horizontal line

¹For large n , we have $P(a_j \in B_1 \wedge a_j \in B_2) = P(a_j \in B_1)P(a_j \in B_2) = (1 - \frac{1}{e})^2 \approx 0.400$

indicates the instability value at the local minimum at $k = 3$ (separately for each method). We see that the unnormalized instability paths intersect this local minimum at $k = 23$ (model free) and $k = 25$ (model based), implying that we would estimate \hat{k} incorrectly, if we were to consider k s larger than 23 or 25, respectively. For more complex clustering problems this behavior of cluster instability may occur much earlier. In sum, if we consider an unconstrained range of k , the unnormalized instability approach will lead to incorrect estimates of k^* .

Key publications on instability-based methods commonly consider only a limited sequence of k . For instance, Fang and Wang (2012) and Ben-Hur *et al.* (2001) consider $k \in \{2, 3, \dots, 10\}$. Figure 1 shows that considering only a limited k -sequences essentially 'cuts' the tail of the instability path before it drops below its local minimum at k^* . It follows that unnormalized methods can perform well if both k^* is small and one considers only a sequence of small k s. However, the results in Table 2 in Fang and Wang (2012) show that increasing the correlation between features and adding noise dimensions results in a considerable performance drop. This suggests that the clustering instability decays more quickly for harder cluster problems. This would imply that the unnormalized instability path overestimates k even when considering only a sequence of small k s if the clustering problem is sufficiently hard.

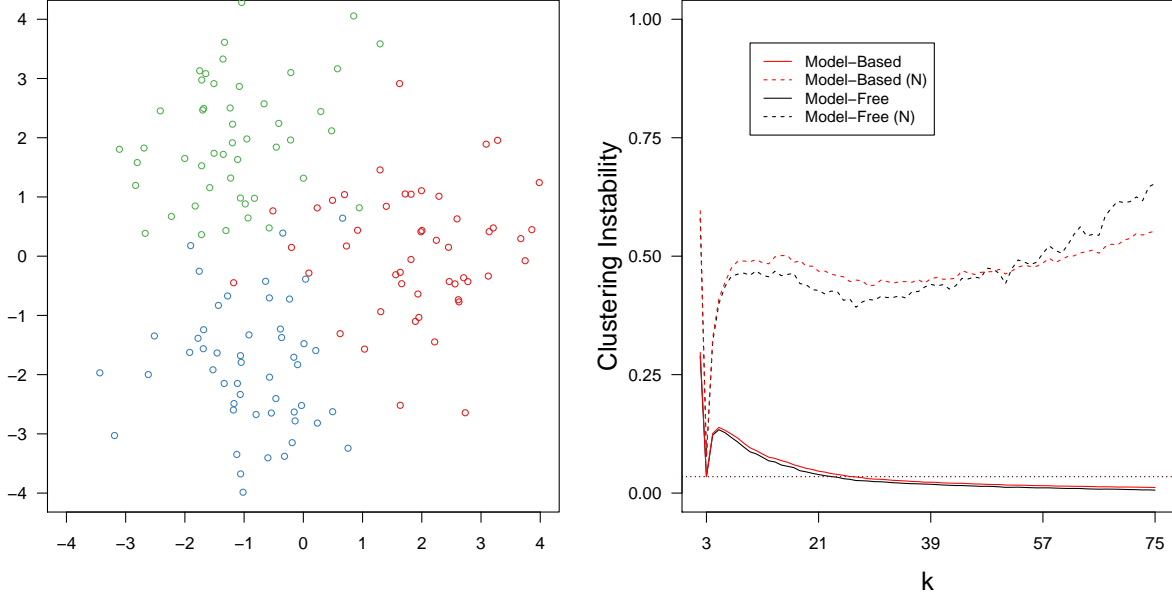


Figure 1: Left: mixture of three (each $n = 50$) 2-dimensional Gaussians with zero covariance and $\sigma_i = 1$. Right: instability path for the model-based (red) and model-free instability approach (black), both normalized (dashed) and unnormalized (solid). The horizontal lines indicate the local minimum of the instability path at $k^* = 3$ for each method. The estimate \hat{k} will be incorrect (too large) if we consider k s with an instability below the corresponding horizontal line.

To overcome this undesirable behavior of the instability path, we introduce a normalization constant that accounts for the trivial decrease in instability due to increasing k . In the rest of this section we show how to compute this normalization constant based on a given k and clustering assignment $\psi(\mathbf{X})$.

Let $M = \{n_1, n_2, \dots, n_K\}$ be the number of objects in each of the clusters in a given clustering $\psi(\mathbf{X})$. We calculate the probability that two objects X_1, X_2 are assigned to the same cluster by chance given the frequencies defined by M . Note that in the model-based approach the sum $\sum_{i=1}^K n_i$ is equal to the number of objects in the original data set \mathbf{X} , whereas in the model-free approach it is equal to the number of objects in the intersection $\tilde{\mathbf{X}}_{\alpha \cap \beta, b}$ of the two bootstrap samples.

We define the probability of two objects being in the same cluster by chance as the ratio of all possible permutations N_{pair} for which X_1, X_2 are in the same cluster and the number of all

possible combinations N_{tot}

$$p[\psi(X_1) = \psi(X_2)] = \frac{N_{pair}}{N_{tot}}. \quad (3)$$

We first compute

$$N_{tot} = \prod_{1 \leq i \leq K} \binom{m_i}{n_i}, \quad (4)$$

where n_i is the number of objects in cluster i and m_i is the number of objects that are not yet contained in already considered clusters

$$m_i = \sum_{i \leq j \leq k} n_j.$$

Intuitively, this computes all possible ways to select n_1 objects from the set of all objects. Then we multiply this quantity by the number of possible ways to select n_2 objects from the set of all objects minus the just selected n_1 objects, etc.

Next, we compute N_{pair}

$$N_{pair} = \sum_{\substack{1 \leq i \leq k \\ n_i \geq 2}} \binom{m-2}{n_i-2} \prod_{\substack{1 \leq j \leq k \\ j \neq i}} \binom{m_j}{n_j}. \quad (5)$$

Here, we assume two objects to be in the same cluster, and analogous to above, compute the number of possible ways to distribute the remaining objects across clusters, while respecting the cluster sizes M .

We can now use (3) to compute the probability of two objects X_1, X_2 being in the same cluster by chance for both clusterings ψ_a, ψ_b . We then plug this probabilities in the definition of clustering distance in terms of probabilities in (1) to obtain $d^r(\psi_a, \psi_b)$, the expected clustering distance under random allocation for a given k and M .

The instability due to chance d^r drives the trivial decrease of clustering instability for larger k . We illustrate this effect in Figure 2 which shows d^r for $k \in \{2, 3, \dots, 100\}$ and various $M \sim \text{Multinomial}(\theta)$ with $\theta \sim \text{Dirichlet}(1)$. We see a clear decrease in d^r , as well as considerable variation due to variation in M , suggesting a complex relationship between M, k , and d^r . As our normalization is based directly on M , our approach not only accounts for the decrease for larger k , but also the effect associated with M .

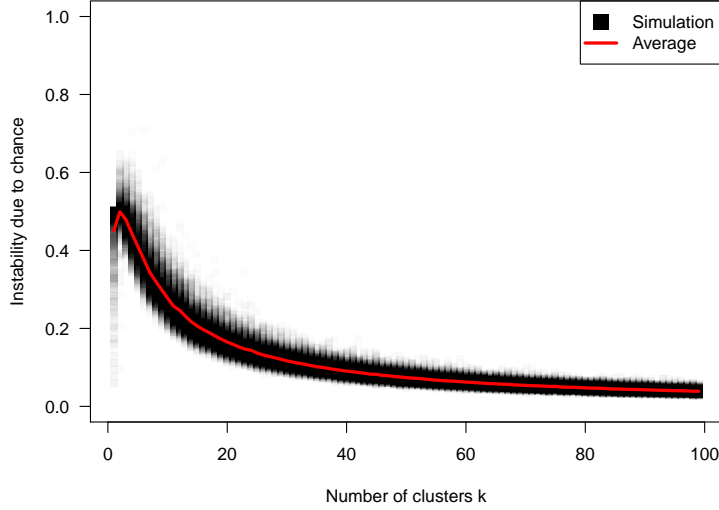


Figure 2: Instability due to chance for randomly generated M for $k \in \{1, \dots, 100\}$. Simulation is based on calculating instability for sets of M generated by randomly distributing 100 objects across k clusters. The shaded squares in the background show the distribution in d^r only due to variation in M for a given k .

To normalize the original cluster distance with d^r we calculate

$$d^n(\psi_a, \psi_b) = \frac{d(\psi_a, \psi_b)}{d^r(\psi_a, \psi_b)} \quad (6)$$

to remove the effect of change clustering instability for larger k (and variation in M). Figure 2 demonstrates the impact of our normalization approach: while the normalized stability paths (dashed line) also exhibit a local minimum at $k = 3$, they do not decrease for larger k . Thus, in this case, our normalization renders the local minimum global, facilitating consistent estimation of k^* via (2).

Note that the exact relationship between $d^r(\psi_a, \psi_b)$ and k not only depends on M , but also the data generating mechanism \mathcal{P} and the clustering algorithm. While our numerical experiments demonstrate the usefulness of accounting for $d^r(\psi_a, \psi_b)$ due to k and M , we leave it to future work to uncover the potentially complex effects and interactions of all of the components of $d^r(\psi_a, \psi_b)$.

6 Numerical experiments

We now turn to numerical evaluation of the performance of unnormalized and normalized instability-based methods across four scenarios. This will include a comparison of the both instability-based approaches to the performance of four popular distance-based methods for selecting k^* .

6.1 Data generation

We generate data from Gaussian mixtures as illustrated in Figure 3. For the first scenario with $k^* = 3$, we distributed the means of three Gaussians with $\sigma = .15$ arranged on a unit circle. The second scenario adapts the first by setting $k^* = 7$ and $\sigma = .04$. We chose prime numbers and a circular layout to avoid local minima for $k < k^*$. The third and fourth scenario used elongated clusters similar to those in Tibshirani and Walther (2005): we generated $n = 50$ equally spaced points along the diagonal of a 3-dimensional cube with side length $[-5, 5]$, and added uncorrelated Gaussian noise ($\mu = 0$ and $\sigma_i = 0.1$) to each data point. We then copy these data points $k^* = 3$ (scenario 3) or $k^* = 7$ (scenario 4) times and place them along the same line separated by a distance of 15. Columns three and four in Figure 3 illustrate these elongated clusters in the first two dimensions, respectively.

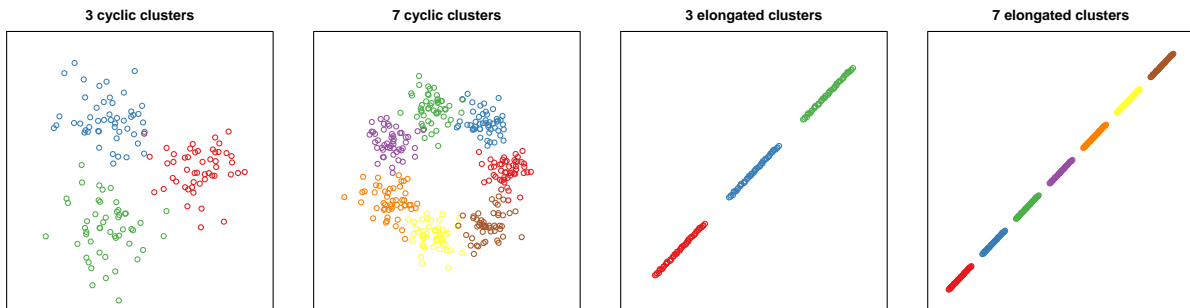


Figure 3: First column: three Gaussians with $\sigma = .1$ and $n = 50$ placed on a circle; second column: seven Gaussians with $\sigma = .04$ and $n = 50$ placed on a circle; third column: three elongated clusters in three dimensions (only the first 2 shown); fourth column: seven elongated clusters in three dimensions (only the first 2 shown).

6.2 Comparison plan

The main contribution of this paper is to improve existing stability-based methods. Our numerical experiments will thus focus on whether our methods based on normalized clustering instability outperform the previously proposed stability-based methods.

To also learn about the relative merits of stability-based methods, we compare their performance to the performance of popular distance-based methods for k^* -selection. Note that these methods imply different definitions of a 'good' clustering (see introduction). Thus, strictly speaking the different methods solve different problems. Nonetheless, in practice, all of these methods are applied for the same purpose. In this context, the various methods can be understood as different heuristics solutions to a given problem (here the 4 scenarios described in Section 6.1).

We consider the following four distance-based methods: the Gap Statistic (Tibshirani *et al.*, 2001), the Jump statistic (Sugar and James, 2011), the the Silhouette statistic (Rousseeuw, 1987), the Slope statistic (Fujita *et al.*, 2014), and a Gaussian mixture model. The Gap statistic simulates uniform data of the same dimensionality as the original data and then compares the gap between the logarithm of the within-cluster dissimilarity $W(k)$ for the simulated and original data. It selects the k for which this gap is largest. The Jump statistic computes the differences of the within-cluster distortion at k and $k - 1$ (after transformation via a negative power) to select k that produced the largest differences in distortions. The Slope statistic is based on the Silhouette statistic $Si()$, and selects k to maximize $[Si(k) - Si(k - 1)]Si(k)^v$, where v is a tuning parameter. Finally, the Gaussian mixture model selects k as the number of components in the mixture model yielding the lowest Bayesian Information Criterion (BIC) (Schwarz *et al.*, 1978).

6.3 Results

We evaluated the k -selection methods using the k-means clustering algorithm (Hartigan, 1975). The k-means algorithm was restarted 10 times with random starting centroids in order to avoid local minima. For all methods, we considered the sequence $k = \{2, 3, \dots, 50\}$. For the stability-based methods we use 100 bootstrap comparisons (see Algorithm 1 and 2). To maximize comparability, we evaluated used the same random seed for all instability-based methods (within the same iteration).

		3 circular clusters, 2 dimensions																		
		2	3	4	5	6	7	8	9	10	11	12	13	14	15	16	17	18	19	20+
Model-based	0	68	0	0	0	0	0	0	0	0	0	0	0	0	0	0	0	0	0	32
Model-based (N)	0	100	0	0	0	0	0	0	0	0	0	0	0	0	0	0	0	0	0	0
Model-free	0	43	0	0	0	0	0	0	0	0	0	0	0	0	0	0	0	0	0	57
Model-free (N)	0	100	0	0	0	0	0	0	0	0	0	0	0	0	0	0	0	0	0	0
Gap Statistic	0	100	0	0	0	0	0	0	0	0	0	0	0	0	0	0	0	0	0	0
Jump Statistic	0	0	0	0	0	0	0	0	0	0	0	0	0	0	0	0	0	0	0	100
Slope Statistic	0	96	4	0	1	0	0	0	0	0	0	0	0	0	0	0	0	0	0	0
Gaussian Mixture	0	100	0	0	0	0	0	0	0	0	0	0	0	0	0	0	0	0	0	0

		7 circular clusters, 2 dimensions																		
		2	3	4	5	6	7	8	9	10	11	12	13	14	15	16	17	18	19	20+
Model-based	0	0	0	0	0	0	0	0	0	0	0	0	0	0	0	0	0	0	0	100
Model-based (N)	0	0	0	0	0	87	13	0	0	0	0	0	0	0	0	0	0	0	0	0
Model-free	0	0	0	0	0	0	0	0	0	0	0	0	0	0	0	0	0	0	0	100
Model-free (N)	0	0	0	0	0	91	9	0	0	0	0	0	0	0	0	0	0	0	0	0
Gap Statistic	0	0	0	0	0	100	0	0	0	0	0	0	0	0	0	0	0	0	0	0
Jump Statistic	0	0	0	0	0	8	0	0	0	0	0	0	0	0	0	0	0	0	0	92
Slope Statistic	0	0	0	0	0	31	17	18	18	9	5	1	0	0	1	0	0	0	0	0
Gaussian Mixture	0	0	0	0	0	99	1	0	0	0	0	0	0	0	0	0	0	0	0	0

		3 elongated clusters, 2 dimensions																		
		2	3	4	5	6	7	8	9	10	11	12	13	14	15	16	17	18	19	20+
Model-based	0	100	0	0	0	0	0	0	0	0	0	0	0	0	0	0	0	0	0	0
Model-based (N)	0	100	0	0	0	0	0	0	0	0	0	0	0	0	0	0	0	0	0	0
Model-free	0	100	0	0	0	0	0	0	0	0	0	0	0	0	0	0	0	0	0	0
Model-free (N)	0	100	0	0	0	0	0	0	0	0	0	0	0	0	0	0	0	0	0	0
Gap Statistic	0	0	0	0	0	0	0	0	0	0	0	0	0	0	0	0	0	0	0	100
Jump Statistic	0	0	0	0	0	0	0	0	0	0	0	0	0	0	0	0	0	0	0	100
Slope Statistic	0	100	0	0	0	0	0	0	0	0	0	0	0	0	0	0	0	0	0	0
Gaussian Mixture	0	99	0	0	1	0	0	0	0	0	0	0	0	0	0	0	0	0	0	0

		7 elongated clusters, 2 dimensions																		
		2	3	4	5	6	7	8	9	10	11	12	13	14	15	16	17	18	19	20+
Model-based	0	0	0	0	0	0	0	0	0	0	0	0	0	0	0	0	0	0	0	100
Model-based (N)	24	0	0	0	0	38	38	1	1	0	0	0	0	0	0	0	0	0	0	0
Model-free	0	0	0	0	0	0	0	0	0	0	0	0	0	0	0	0	0	0	0	100
Model-free (N)	24	0	0	0	0	47	29	0	0	0	0	0	0	0	0	0	0	0	0	0
Gap Statistic	0	0	0	0	0	0	0	0	0	0	0	0	0	0	0	0	0	0	0	100
Jump Statistic	0	0	0	0	0	0	0	0	0	0	0	0	0	0	0	0	0	0	0	100
Slope Statistic	0	0	0	0	0	68	7	10	6	2	4	3	0	0	0	0	0	0	0	0
Gaussian Mixture	0	0	0	0	0	100	0	0	0	0	0	0	0	0	0	0	0	0	0	0

Table 1: Estimated number of clusters in four different scenarios for 100 iterations.

Table 1 shows the estimated \hat{k} over 100 iterations for each of the four scenarios and eight methods. Estimated $\hat{k} \geq 20$ are collapsed in the category '20+'. We first focus on the results of the instability-based methods. For the first scenario with $k^* = 3$ circular clusters, the unnormalized instability-based methods perform poorly, with about half of the estimates being correct, and the other half being in the category '20+'. This poor performance is due to the unfavorable behavior illustrated in Figure 2 and Figure 1. The normalized instability methods, however, do not suffer from this problem and accordingly show high performance. The pattern of results in the scenario with $k^* = 7$ is similar, but more pronounced. With the clustering problem being more difficult, unnormalized stability methods fail to identify k^* in every iteration, whereas the normalized stability methods still successfully identify k^* in the vast majority of cases. In scenario three with $k^* = 3$ elongated clusters all instability-based methods show maximum performance. Here the tail of the unnormalized instability paths decays slowly enough preventing the trivial decrease instability to undercut the local minimum at $k = 3$. In scenario four with $k^* = 7$ elongated clusters, the performance of the unnormalized methods drops to zero, whereas normalized instability methods are still able to identify k^* in a considerable amount of cases. Overall the results show that the normalized instability-methods perform better than the unnormalized ones.

We now turn to the performance of distance-based methods. The clear winner among this class of methods is the Gaussian mixture, which performs extremely well in all scenarios. Next, the Slope statistic performs reasonably well, however, the performance is much lower for $k^* = 7$ than for $k^* = 3$. The Gap statistic shows maximal performance for the circular clusterings, but drops to zero in for the elongated clusters. Finally, the Jump statistic fails entirely in all scenarios. The reason for the bad performance of the Jump statistic is that its variance increases with increasing k . See Appendix B for a detailed illustration of this problem.

Comparing stability- and distance-based methods, we find that stability-based methods perform rather well. When using our proposed normalization, stability-based methods outperform every distance-based method, except for the Gaussian mixture methods. However, when using the unnormalized methods, it is almost always better to use any of the distance-based methods. For additional comparisons between the methods, consult Appendix A where we study small variations of scenario one and two including additional noise dimensions.

Another noteworthy finding of our analysis is the near-equivalent performance of the model-

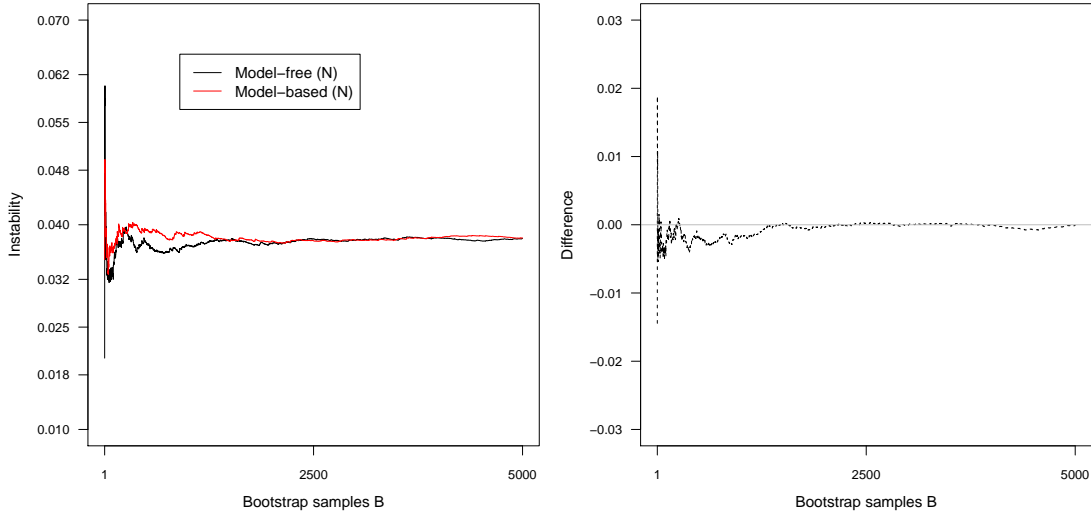


Figure 4: Left: The average instability for fixed $k = 3$ up to bootstrap sample b for both the model-based (red) and model-free (black) instability approach. The data is the one from in Figure 1. Right: The difference between the two functions.

based and the model-free instability approaches (see Table 1). To analyze whether the two methods would produce equivalent results in the long run, we analyzed the methods using the scenario of Figure 1) over a increasing number of $B \in \{1, 2, \dots, 5000\}$ bootstrap comparisons.

Figure 4 (left) shows that both methods seem to stabilize in a small region around .038. However from the average difference (right) it is unclear whether the two methods converge.

Note that right differences between the two instabilities (right panel in Figure 4) become small, but they do not approach zero. Furthermore, we evaluated the correlation between the instability paths of both approaches for the simulation reported in Table 1. They are between .98 and 1, suggesting that the two methods show very similar performance.

7 Conclusions

We proposed a normalization for instability-based methods for the estimation of k^* that permits successful identification k^* for arbitrarily large sequences of k . This improves upon existing methods which only show good performance when constraining the range candidate k to small values, e.g., $k \in \{2, 3, \dots, 10\}$.

We also showed that instability-based methods, especially when using the proposed normalization, outperform several established distance-based k -selection methods. In addition, we showed that the performance of the model-based and model-free variants of the instability-based method are similar, but not identical. It seems worthy to pursue formalization of the relationship between the two variants in future research.

Acknowledgements

We would like to thank Junhui Wang for helpful answers to several questions about his papers on clustering instability. This project was supported by the European Research Council Consolidator Grant no. 647209.

References

- Ben-Hur, A., Elisseeff, A., and Guyon, I. (2001). A stability based method for discovering structure in clustered data. In *Pacific symposium on biocomputing*, volume 7, pages 6–17.
- Bengio, Y., Vincent, P., Paiement, J.-F., Delalleau, O., Ouimet, M., and Le Roux, N. (2003). *Spectral clustering and kernel PCA are learning eigenfunctions*, volume 1239. Citeseer.
- Fang, Y. and Wang, J. (2012). Selection of the number of clusters via the bootstrap method. *Computational Statistics & Data Analysis*, **56**(3), 468–477.
- Friedman, J., Hastie, T., and Tibshirani, R. (2001). *The elements of statistical learning*, volume 1. Springer series in statistics Springer, Berlin.
- Fujita, A., Takahashi, D. Y., and Patriota, A. G. (2014). A non-parametric method to estimate the number of clusters. *Computational Statistics & Data Analysis*, **73**, 27–39.
- Hartigan, J. A. (1975). *Clustering algorithms*.
- Hennig, C. (2007). Cluster-wise assessment of cluster stability. *Computational Statistics & Data Analysis*, **52**(1), 258–271.
- Hennig, C. (2015). What are the true clusters? *Pattern Recognition Letters*, **64**, 53–62.

- Ng, A. Y., Jordan, M. I., Weiss, Y., *et al.* (2002). On spectral clustering: Analysis and an algorithm. *Advances in neural information processing systems*, **2**, 849–856.
- Rousseeuw, P. J. (1987). Silhouettes: a graphical aid to the interpretation and validation of cluster analysis. *Journal of computational and applied mathematics*, **20**, 53–65.
- Schwarz, G. *et al.* (1978). Estimating the dimension of a model. *The annals of statistics*, **6**(2), 461–464.
- Sugar, C. A. and James, G. M. (2011). Finding the number of clusters in a dataset. *Journal of the American Statistical Association*.
- Tibshirani, R. and Walther, G. (2005). Cluster validation by prediction strength. *Journal of Computational and Graphical Statistics*, **14**(3), 511–528.
- Tibshirani, R., Walther, G., and Hastie, T. (2001). Estimating the number of clusters in a data set via the gap statistic. *Journal of the Royal Statistical Society: Series B (Statistical Methodology)*, **63**(2), 411–423.
- Wang, J. (2010). Consistent selection of the number of clusters via crossvalidation. *Biometrika*, **97**(4), 893–904.

A Additional Numerical Experiments

We show the results of two additional scenarios that are adapted from scenarios one and two in Section 6.3 by adding eight dimensions of uncorrelated Gaussian noise with standard deviations $\sigma = .15$ in scenario one and $\sigma = .04$ in scenario two.

3 circular clusters, 10 dimensions

	2	3	4	5	6	7	8	9	10	11	12	13	14	15	16	17	18	19	20+
Model-based	0	49	0	0	0	0	0	0	0	0	0	0	0	0	0	0	0	0	51
Model-based (N)	0	100	0	0	0	0	0	0	0	0	0	0	0	0	0	0	0	0	0
Model-free	0	4	0	0	0	0	0	0	0	0	0	0	0	0	0	0	0	0	96
Model-free (N)	0	100	0	0	0	0	0	0	0	0	0	0	0	0	0	0	0	0	0
Gap Statistic	0	100	0	0	0	0	0	0	0	0	0	0	0	0	0	0	0	0	0
Jump Statistic	0	0	0	0	0	0	0	0	0	0	0	0	0	0	0	0	0	0	100
Slope Statistic	0	97	3	0	0	0	0	0	0	0	0	0	0	0	0	0	0	0	0
Gaussian Mixture	0	100	0	0	0	0	0	0	0	0	0	0	0	0	0	0	0	0	0

7 circular clusters, 10 dimensions

	2	3	4	5	6	7	8	9	10	11	12	13	14	15	16	17	18	19	20+
Model-based	0	0	0	0	0	0	0	0	0	0	0	0	0	0	0	0	0	0	100
Model-based (N)	0	0	0	0	0	68	32	0	0	0	0	0	0	0	0	0	0	0	0
Model-free	0	0	0	0	0	0	0	0	0	0	0	0	0	0	0	0	0	0	100
Model-free(N)	0	0	0	0	0	83	17	0	0	0	0	0	0	0	0	0	0	0	0
Gap Statistic	0	0	0	0	0	100	0	0	0	0	0	0	0	0	0	0	0	0	0
Jump Statistic	0	0	0	0	0	0	0	0	0	0	0	0	0	0	0	0	0	0	100
Slope Statistic	0	9	91	0	0	0	0	0	0	0	0	0	0	0	0	0	0	0	0
Gaussian Mixture	0	0	0	0	0	100	0	0	0	0	0	0	0	0	0	0	0	0	0

Table 2: Estimated number of clusters in different scenarios

The performance is qualitatively similar to the performance reported in the main text. However, performance dropped for all methods as a result of the added noise, which rendered the clustering problem more difficult.

B Path of Jump Statistic

One reason for the bad performance of the Jump statistic is that the variance of the jump size increasing as k increases. We illustrate this problematic behavior of the jump statistic in Figure 5 using 100 iterations of scenario one (three circular clusters) and two (seven circular clusters) from the main text.

The figure plots are the paths Jump statistic for each of the 100 iterations across $k \in \{2, 3, \dots, 10\}$.

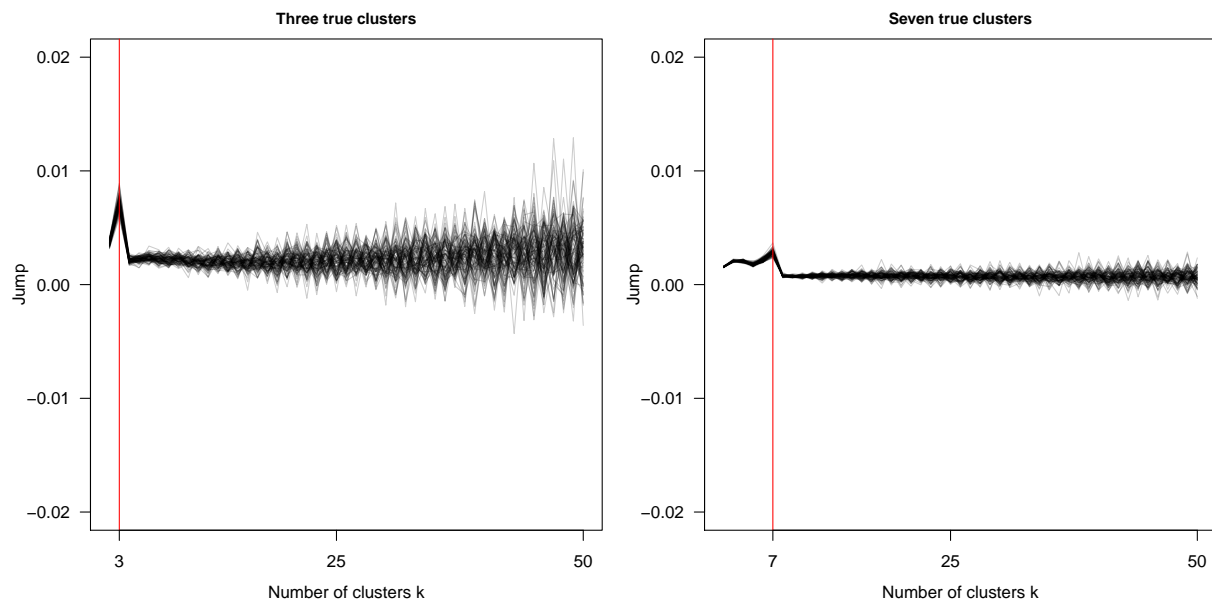


Figure 5: The jump-path along the sequence of considered k for each of the 100 simulation iterations. Left: for the scenario with 3 true clusters in 2 dimensions. Right: for the scenario with 7 true clusters in 2 dimensions.

We see that the variance of the Jump statistic paths clearly increases for larger k . This implies that similarly to the unnormalized stability-based methods, the Jump statistic can only identify k^* , when the range of possible k is restricted to a small range around the true k^* .